

Jaime J. L. Quispe, Tarcisio F. Maciel, Yuri C. B. Silva, Anja Klein, “Joint Beamforming and BS Selection for Energy-Efficient Communications via Aerial-RIS,” in *Proc. IEEE Global Communications Conference Workshops (Globecom Workshops)*, December 2021.

©2021 IEEE. Personal use of this material is permitted. However, permission to reprint/republish this material for advertising or promotional purposes or for creating new collective works for resale or redistribution to servers or lists, or to reuse any copyrighted component of this works must be obtained from the IEEE.

Joint Beamforming and BS Selection for Energy-Efficient Communications via Aerial-RIS

Jaime J. L. Quispe*, Tarcisio F. Maciel[◊], Yuri C. B. Silva[◊] and Anja Klein*

*Communications Engineering Lab, Technische Universität Darmstadt, Germany. Email: {j.luque, a.klein}@nt.tu-darmstadt.de

[◊]Wireless Telecom Research Group (GTEL), Federal University of Ceará, Brazil. Email: {maciel, yuri}@gtel.ufc.br

Abstract—Cooperative BS transmission via unmanned aerial vehicles (UAVs)-airborne reconfigurable intelligent surface (RIS), also known as aerial-RIS, is a promising solution for providing connectivity in emergency areas where network access is unavailable. The RIS requires low power in reflecting the impinging base station (BS) signals towards the direction of the user equipment (UE), and the cooperative transmission can provide a more stable connection that guarantees quality-of-service (QoS). In this work, we investigate the energy efficiency (EE) maximization of a multiple-BS single-UE single-aerial-RIS setup and the usefulness of cooperation to prevent outages. The BSs can be turned either on or off depending on their contribution to the EE, and the system is subject to QoS, power, capacity, and RIS specific constraints. We formulate a problem that jointly optimizes the selection of the BSs and the beamforming weights of BSs and RIS, and solve it with a Branch-Reduce-and-Bound (BRnB) algorithm that uses monotonic optimization and semidefinite relaxation steps. Simulation results for an illustrative setup show that the aerial-RIS increases the EE by 50% when doubling the number of its elements and cooperative aerial-RIS transmissions help to solve outages of single-BS cases.

Index Terms—UAV-communications, reconfigurable intelligent surfaces, energy efficiency, beamforming, monotonic optimization, semi-definite relaxation.

I. INTRODUCTION

Responding to emergency situations where a communication infrastructure is either unavailable or destroyed by a natural disaster requires an easy-to-deploy and cost-effective radio access for information sharing and coordination between first responders and the affected people (see earthquake in Peru in 2007, and floods in Brasil in 2019 and Germany in 2021). It is also often necessary to run diverse wireless applications, for instance, to provide connectivity to individual user equipments (UEs) in confined areas, such as a trapped firefighter, a person's vital signs monitor or a remote-controlled rescue robot. In these cases, using an unmanned aerial vehicle (UAV) equipped with a base station (BS) can be a temporary solution due to its fast and flexible deployment [1]. However, carrying and operating the BS can reduce the energy available for the rest of its functions, as well as the channel path loss can impact the performance [2]. On the other

This work has been performed in the context of the LOEWE Center emergenCITY, the BMBF project Open6GHub, and has been supported by DAAD with funds from the German Federal Ministry of Education and Research (BMBF). T. F. Maciel and Y. C. B. Silva also acknowledge the support of CNPq and CAPES/PROBRAL Grant 88887.144009/2017-00. We thank Dr. Lin Xiang for the fruitful discussions and comments.

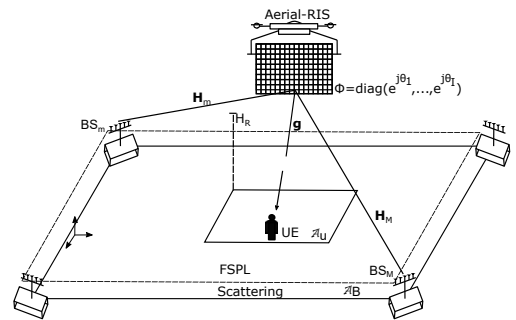


Fig. 1. Aerial-RIS-aided cooperative wireless communication system

hand, reconfigurable intelligent surfaces (RISs)-aided links are energy-efficient alternatives to increase channel gains, and thus increase the data rate and reduce the power consumption of the communication system [3]. An RIS operates by inserting phase shifts to the signals impinging on its surface such that they are reflected in desired directions, and coherently added at the receivers. A UAV airborne RIS, also known as an aerial-RIS, eliminates the use of power amplifiers (PAs) and signal processing units, which reduces the power required for carrying communication equipment onboard, and also enables three-dimensional signal reflections from the sky [4]. In order to guarantee the quality-of-service (QoS) of the application, BS cooperative transmission can be used to set a stable BS-RIS-UE connection. Moreover, new fabrication technologies [5] might reduce the weight of RISs so that they can be mounted on drones. Due to the interesting advantages and challenges of the cooperative aerial-RIS setup, this work aims to assess its EE performance.

A. Related works

An application example of an aerial-RIS to assist the communication between one UE and one BS is studied in [4], which iteratively optimizes the BS and RIS beamformers, and the UAV placement for maximum signal-to-noise ratio (SNR). It shows that the SNR increases by 6 dB when doubling the number of RIS elements. For the same application, the work in [6] addresses the aerial-RIS in a multi-BS scenario and shows that even if the BS transmit powers increase, this does not translate to a higher SNR level if the phase-shifts are not optimized. Regarding the UAV-UE propagation channel, the study in [2] shows that it can be modeled as a

composition of free space propagation with high line-of-sight (LoS) probability plus random scattering and shadowing due to ground structures surrounding the UE and the BS. Based on an outage probability (OP) predictor for an aerial-RIS single-BS setup, the work in [7] shows that the power needed to achieve a target OP is reduced with the number I of RIS elements. For example, it drops by 8.2 dB when doubling I from 15 to 30 for an OP of 0.01. Then it concludes that the EE is also improved. Furthermore, the authors showed that this setup outperforms several dual-hop relay schemes.

In comparison to terrestrial RIS setups, where an EE gain of a factor of 3 w.r.t. an Amplify-and-Forward (AF) relay was obtained [3], studies for EE in aerial-RIS systems are scarce. Also, there are only a few works devoted to optimal solutions for the RIS or multiple-BS beamforming, as for example the algorithms in [8] and [9] for SNR and EE maximization, respectively. Finally, regarding RIS implementation, it has been studied that the degree of adjustment of the phase-shifts depends on the antenna circuits impedance [5].

B. Scope and contributions

We investigate the EE of an aerial-RIS-aided network for disaster relief where a number of geographically distributed UAV ground control stations, each with a BS, cooperatively create downlinks to the UE located in a remote area without coverage. This scenario is illustrated in Fig. 1. We consider that the BSs are turned on depending on the communication requirement and its contribution to the EE, otherwise they are put into a sleep mode of low power consumption. We optimize which BSs should be selected to serve the UE jointly with the BS and RIS beamformers for maximum EE which, as far as we know, has not been studied before. We also consider QoS, fronthaul capacity, and power constraints, as well as constraints on the range of values of the possible RIS reflection phases, which come from hardware implementation [5]. The formulated EE problem is verified to be non-convex and is solved by using discrete monotonic optimization (MO) [10] and semidefinite relaxation (SDR) [11] methods.

C. Paper outline and notation

Section II introduces the system model of the aerial-RIS-aided communication system, including the models for power consumption, BS activations and fronthaul capacity, as well as the problem formulation. Section III addresses the development of the optimization algorithm. Section IV presents the simulation results and Section V concludes this paper.

We use the following notations: bold lower case, bold upper case and calligraphic letters denote vectors, matrices, and sets, respectively. $(\cdot)^T$, $(\cdot)^H$, $\|\cdot\|$, $\text{diag}(\cdot)$, $\arg(\cdot)$, $\text{tr}(\cdot)$, denote the transpose, Hermitian, Euclidean norm, diagonal, argument and trace operators. For any vector \mathbf{v} , v_i represents its i th element and if \mathbf{v} and $\mathbf{z} \in \mathbb{R}^N$, $\mathbf{v} \leq \mathbf{z}$ means $v_i \leq z_i, \forall i$. A box is expressed as $[\mathbf{x}, \mathbf{z}]$, where any vector \mathbf{y} within the box satisfies $\mathbf{x} \leq \mathbf{y} \leq \mathbf{z}$. The set of positive semidefinite $n \times n$ matrices is denoted by \mathcal{S}_+^n and given two $n \times n$ matrices \mathbf{A} and \mathbf{B} , $\mathbf{A} \succeq \mathbf{B}$ means $(\mathbf{A} - \mathbf{B}) \in \mathcal{S}_+^n$. The floor and ceil rounded

values of a number x on a set \mathcal{D} are denoted as $\lfloor x \rfloor_{\mathcal{D}}$ and $\lceil x \rceil_{\mathcal{D}}$, respectively, whereas $\lfloor \mathbf{x} \rfloor_{i/\mathcal{D}}$ and $\lceil \mathbf{x} \rceil_{i/\mathcal{D}}$ are vectors of which only the i th element is rounded. \mathbf{e}_i is a vector such that $e_i = 1$ and $e_j = 0, \forall j \neq i$.

II. SYSTEM MODEL AND PROBLEM FORMULATION

A. Scenario

The communication scenario consists of M base stations, each with N antennas, that aim to serve a ground single-antenna UE via one aerial-RIS as presented in Fig. 1. The BS transmissions are in the same time-frequency resources. The RIS is equipped with I antenna elements with configurable phase-shifts of unit-amplitude for reflecting the incoming BS signals towards the direction of the UE. We consider that the downlink UE data d , which has unit variance, is available at the BSs, which are connected via fronthaul links to a CPU. From information about the channel responses, the CPU calculates the BS and RIS beamformers and BS activation decisions in order to meet QoS requirements. Each BS is indexed by $m \in \mathcal{M} \triangleq \{1, \dots, M\}$ and for every BS, $\mathbf{w}_m \in \mathbb{C}^{N \times 1}$ and $\mathbf{H}_m \in \mathbb{C}^{I \times N}$ denote its beamforming vector and its channel to the RIS, respectively. The RIS-UE channel is denoted by $\mathbf{g} \in \mathbb{C}^{1 \times I}$. Therefore, the equivalent channel between the UE and the BSs can be modeled by $\mathbf{h}(\phi) \triangleq \mathbf{g}\Phi\mathbf{H} \in \mathbb{C}^{1 \times MN}$, where $\mathbf{H} \triangleq [\mathbf{H}_1, \dots, \mathbf{H}_M]$, $\Phi \triangleq \text{diag}(\phi)$, and $\phi \triangleq [e^{j\theta_1}, \dots, e^{j\theta_I}]^T$, with θ_i being the phase shift at RIS antenna $i \in \mathcal{I} \triangleq \{1, \dots, I\}$. If $\mathbf{w} \triangleq [\mathbf{w}_1^T, \dots, \mathbf{w}_M^T]^T$ denotes the composite beamforming vector, and $n \sim \mathcal{CN}(0, \sigma^2)$ is the noise of variance σ^2 , the received signal can be modeled as $y = \mathbf{h}\mathbf{w}d + n$, and the SNR as

$$\gamma(\mathbf{w}, \phi) = \frac{|\mathbf{h}\mathbf{w}|^2}{\sigma^2}. \quad (1)$$

Therefore, the spectral efficiency (SE) is

$$r(\mathbf{w}, \phi) = \log_2(1 + \gamma(\mathbf{w}, \phi)) \text{ bit/s/Hz}. \quad (2)$$

B. Fronthaul capacity

We represent the activation of BS m for serving the UE by a variable $s_m \in \mathcal{B} \triangleq \{0, 1\}$ and assume that the fronthaul rate of each BS to the CPU c_m is limited by a maximum capacity \bar{C}_m , i.e.,

$$c_m = s_m r(\mathbf{w}, \phi) \leq \bar{C}_m \text{ bit/s/Hz}, \quad \forall m \in \mathcal{M}. \quad (3)$$

We consider that several digital signal processing (DSP) tasks as encoding, beamforming and fronthauling are performed at the CPU and consume a power that depends on the fronthaul rate as

$$p_{\text{DSP}} = \eta_{\text{FH}} \sum_{m \in \mathcal{M}} c_m, \quad (4)$$

where η_{FH} is a constant factor in W/Gbit/s/Hz.

C. Hardware power consumption

Each BS m has two operational modes selectable by s_m , where $s_m = 1$ indicates an active mode with power consumption $P_{\text{BS}}^{\text{run}}$ from its hardware components, such as microprocessors, memory and backhaul circuitry, and $s_m = 0$ indicates its sleep low power consumption mode with power $P_{\text{BS}}^{\text{sl}}$ [9], [12]. Also, if P_E is the power spent by the RIS antenna circuitry, the hardware power consumption is

$$p_{\text{HW}} = \sum_{m \in \mathcal{M}} (s_m P_{\text{BS}}^{\text{run}} + (1 - s_m) P_{\text{BS}}^{\text{sl}}) + IP_E. \quad (5)$$

D. Radiated power

We assume that the transmit signal power from each BS is limited by \bar{P}_m , i.e. ,

$$\|\mathbf{w}_m\|^2 \leq \bar{P}_m, \quad \forall m \in \mathcal{M} \quad (6)$$

and by assuming PAs of constant efficiency η_{PA} , the power spent for radiation can be expressed as

$$p_{\text{RAD}_m} = \frac{1}{\eta_{\text{PA}}} \|\mathbf{w}_m\|^2, \quad \forall m \in \mathcal{M}. \quad (7)$$

Thus, the total power consumption can be modeled as

$$\begin{aligned} p(\mathbf{s}, \mathbf{w}, \phi) &= p_{\text{DSP}} + p_{\text{HW}} + \sum_{m \in \mathcal{M}} p_{\text{RAD}_m} \\ &= \eta_{\text{FH}} r(\mathbf{w}, \phi) \sum_{m \in \mathcal{M}} s_m + \sum_{m \in \mathcal{M}} s_m \Delta P + \\ &\quad \frac{1}{\eta_{\text{PA}}} \sum_{m \in \mathcal{M}} \|\mathbf{w}_m\|^2 + P_{\text{const}}, \end{aligned} \quad (8)$$

with $\mathbf{s} \triangleq [s_1, \dots, s_M]$, $P_{\text{const}} \triangleq MP_{\text{BS}}^{\text{sl}} + IP_E$ and $\Delta P \triangleq P_{\text{BS}}^{\text{run}} - P_{\text{BS}}^{\text{sl}}$.

E. BS selection

In order to guarantee the application QoS, at least one BS has to be selected to transmit to the RIS and serve the UE and thus put into active mode. Otherwise, the BSs that are not selected can stay in sleep mode to save energy, so that

$$\sum_{m \in \mathcal{M}} s_m \geq 1. \quad (9)$$

F. Problem formulation

The EE maximization problem can be formulated as

$$\mathcal{P}_1 : \eta^* = \max_{\phi, \mathbf{w}, \mathbf{s}} \frac{r(\mathbf{w}, \phi)}{p(\mathbf{s}, \mathbf{w}, \phi)}, \quad (10)$$

$$\text{s.t.}: r(\mathbf{w}, \phi) \geq r_o, \quad (11)$$

$$\|\mathbf{w}_m\|^2 \leq s_m \bar{P}_m, \quad \forall m \in \mathcal{M}, \quad (12)$$

$$|\phi_i| = 1, \quad \forall i \in \mathcal{I}, \quad (13)$$

$$\arg\{\phi_i\} \in \mathcal{F}_i, \quad \forall i \in \mathcal{I}, \quad (14)$$

$$\mathbf{s} \in \mathcal{B}^M, \quad (15)$$

$$(3), (9),$$

where η^* is the optimal EE with unit bit/J/Hz. Constraint (11) is to guarantee an SE of at least r_o bit/s/Hz. In (12), if the BS m is not selected ($s_m = 0$), it does not need to transmit. The unit-modulus and argument constraints for the RIS phase-shifts are given by (13) and (14), respectively, where $\mathcal{F}_i \triangleq [\psi_i^l, \psi_i^u] \subseteq [0, 2\pi]$ is the continuous set for the

phases θ_i . Since the utility function is not jointly concave, the constraints (11) and (13) are non-convex, and the boolean variable \mathbf{s} is mixed with the continuous variables in (3), (10), and (12), we can conclude that \mathcal{P}_1 is a non-convex mixed-boolean non-linear problem (MBNLP). Even though \mathcal{P}_1 is untractable via Dinkelbach or fractional programming transformations, (3) and (9) are monotonic constraints (m.c.'s) that we can exploit. In the next section, we exhibit the rest of the monotonic structure of \mathcal{P}_1 , manage it via monotonic optimization [10], and apply a custom relaxation method based on [11] to find the optimal RIS phase-shifts. These steps are presented in a Branch-Reduce-and-Bound (BRnB) algorithm.

III. JOINT BEAMFORMING AND BS SELECTION

A. Monotonic optimization

The solution search set of \mathcal{P}_1 is shaped by monotonic mixed-boolean and continuous constraints which can be tackled by monotonicity-based cuts, bounding, and boolean adjustments with BRnB [10]. BRnB can also be applied to the non-convex search region of the RIS phase-shifts by exploring the solution in its relaxed region based on the performance bounds that can be achieved locally. If we replace $\|\mathbf{w}_m\|^2$ by its epigraph $t_m, \forall m \in \mathcal{M}$, in the denominator of (10), and then the utility function by its epigraph η_e , and also introduce an auxiliary variable u in (11), we can reformulate \mathcal{P}_1 as

$$\mathcal{P}_2 : \eta^* = \max_{\eta_e, \phi, \mathbf{w}, \mathbf{s}, u, \mathbf{t}} \eta_e, \quad (16)$$

$$\text{s.t.}: u \geq r_o, \quad (17)$$

$$\log_2(1 + \gamma(\mathbf{w}, \phi)) \geq u, \quad (18)$$

$$\eta_e \hat{p}(\mathbf{s}, u, \mathbf{t}) - u \leq 0, \quad (19)$$

$$\|\mathbf{w}_m\|^2 \leq t_m, \quad \forall m \in \mathcal{M}, \quad (20)$$

$$(3), (9), (12), (13), (14), (15),$$

where $\hat{p}(\mathbf{s}, u, \mathbf{t}) \triangleq \eta_{\text{FH}} u \sum_{m \in \mathcal{M}} s_m + \sum_{m \in \mathcal{M}} s_m \Delta P + \frac{1}{\eta_{\text{PA}}} \sum_{m \in \mathcal{M}} t_m + P_{\text{const}}$. Then, we observe that the objective function (16) is a monotonic increasing function (m.i.f.) on η_e and that constraints (3), (9), (17) and (19) can be expressed as difference of m.i.f.'s that depend on \mathbf{s}, u and \mathbf{t} . If these variables are determined, we can compute the EE as $\eta_e = \frac{u}{\hat{p}(\mathbf{s}, u, \mathbf{t})}$. Thus we can avoid branching on η_e . Let N_d be the number of discrete monotonic (d.m.) variables in \mathbf{s} and N_c , the number of continuous monotonic (c.m.) variables in u and \mathbf{t} . We consider that they belong to an N_s -dimensional box \mathcal{S} , with $N_s = N_d + N_c$, where each vertex corresponds to one variable. Also, we create a super N_t -dimensional box containing both \mathcal{S} and \mathcal{I} . If we express the m.i.f. inequalities as a single difference of two m.i.f.'s $g(\cdot)$ and $h(\cdot)$ [10, Corollary 6], the monotonic structure of \mathcal{P}_2 can be represented as

$$\max_{\mathbf{v}} f(\mathbf{v}) | g(\mathbf{v}) \leq h(\mathbf{v}), \quad \mathbf{v} \in [\underline{\mathbf{p}}, \overline{\mathbf{q}}] \subseteq \mathcal{S}, \quad (v_1, \dots, v_{N_d}) \in \mathcal{B}^{N_d},$$

where $g(\mathbf{v})$ and $h(\mathbf{v})$ are m.i.f.'s on $\mathbf{v} \triangleq [v_1, \dots, v_{N_s}]^T$, which contains the variables \mathbf{s}, u and \mathbf{t} , whose lower bounds (with underline notation) and upper bounds (with overline notation)

are given by $\mathbf{p} \triangleq [\underline{\mathbf{s}}^T, \underline{u}, \underline{\mathbf{t}}^T]^T$ and $\mathbf{q} \triangleq [\bar{\mathbf{s}}^T, \bar{u}, \bar{\mathbf{t}}^T]^T$, respectively. In the following, we briefly describe the branching, reduction, and bounding steps.

1) *Branching*: At each iteration, the largest edge of the chosen box $B = [\mathbf{p}, \mathbf{q}]$ is divided in half. This edge is given by $n = \arg \max_{m=1, \dots, N_s} (q_m - p_m)$. If we define $d \triangleq (q_n - p_n)/2$, the two descendant boxes named as B_- and B_+ are given by

$$B_- = \begin{cases} [\mathbf{p}, [\mathbf{q} - d\mathbf{e}_n]_{n/B}], & \text{if } n \leq N_d, \\ [\mathbf{p}, \mathbf{q} - d\mathbf{e}_n], & \text{if } N_d < n \leq N_s, \end{cases} \quad (21)$$

$$B_+ = \begin{cases} [[\mathbf{p} + d\mathbf{e}_n]_{n/B}, \mathbf{q}], & \text{if } n \leq N_d, \\ [\mathbf{p} + d\mathbf{e}_n, \mathbf{q}], & \text{if } N_d < n \leq N_s. \end{cases}$$

2) *Reduction*: We can remove parts of each descendant box $V = [\mathbf{a}, \mathbf{b}]$ that are not in \mathcal{S} or achieve a local performance below the current best global η_e^{global} as to reduce the search space in the next iterations. The reduction step, here denoted as $f_r(V) = V'$, shrinks a box $V = [\mathbf{a}, \mathbf{b}]$ to a box $V' = [\mathbf{a}', \mathbf{b}']$ without losing any feasible solution (in case it exists in V) [10], i.e., provided that $g(\mathbf{a}) \leq h(\mathbf{b})$, V' contains the points $\mathbf{v}' \in [\mathbf{a}, \mathbf{b}] \cap \mathcal{S}$ that satisfy $f(\mathbf{v}') > \eta_e^{global}$. We can replace \mathbf{a} by \mathbf{a}' , which can be obtained as $\mathbf{a}' = \mathbf{b} - \sum_{n=1}^{N_s} \alpha_n (b_n - a_n) \mathbf{e}_n$, where $\alpha_n = \sup\{\alpha | 0 \leq \alpha \leq 1, g(\mathbf{a}) \leq h(\mathbf{b} - \alpha(b_n - a_n) \mathbf{e}_n), f(\mathbf{b} - \alpha(b_n - a_n) \mathbf{e}_n) \geq \eta_e^{global}\}$ and \mathbf{e}_n is the n th unit vector. Also, \mathbf{b} can be replaced by $\mathbf{b}' = \mathbf{a} - \sum_{n=1}^{N_s} \beta_n (a_n - b_n) \mathbf{e}_n$ with $\beta_n = \sup\{\beta | 0 \leq \beta \leq 1, g(\mathbf{a} - \beta(a_n - b_n) \mathbf{e}_n) \leq h(\mathbf{q}), f(\mathbf{q}) \geq \eta_e^{global}\}$. The values of α_n and β_n can be found via bisection for every $n = 1, \dots, N_s$. Likewise, without loss of optimality, the values of the reduced corners a'_n and b'_n , for $n \leq N_d$, can be rounded to $\lceil a'_n \rceil_B$ and $\lfloor b'_n \rfloor_B$ [10].

3) *Bounding*: Since both the numerator and denominator of η_e are m.i.f.'s on $B = [\mathbf{p}, \mathbf{q}]$, we can calculate a local lower bound (l.b.) and a local upper bound (u.b.) for η_e as

$$\eta_e^{lb}(B) = \frac{\underline{u}}{\hat{p}(\underline{\mathbf{s}}, \bar{u}, \underline{\mathbf{t}})}, \quad (22)$$

$$\eta_e^{ub}(B) = \frac{\bar{u}}{\hat{p}(\underline{\mathbf{s}}, \underline{u}, \underline{\mathbf{t}})}. \quad (23)$$

At each iteration i , we update the best l.b. of η_e , also known as the global l.b., as $\eta_{e,i}^{glb} = \max(\eta_{e,i-1}^{glb}, \eta_e^{lb}(B))$, where $\eta_{e,i-1}^{glb}$ is the highest feasible EE obtained until the previous iteration. Also, in order to reduce the search space defined by the stored boxes, we can eliminate each box B having $\eta_e^{ub}(B) < \eta_{e,i}^{glb}$.

We create an initial box $T_0 \triangleq [\mathbf{a}_0, \mathbf{b}_0]$ s.t. $T_0 \supseteq (\mathcal{S} \cup \mathcal{F})$, where $\mathbf{a}_0 \triangleq [\underline{\mathbf{s}}^T, \underline{u}, \underline{\mathbf{t}}^T, \underline{\boldsymbol{\theta}}^T]$ and $\mathbf{b}_0 \triangleq [\bar{\mathbf{s}}^T, \bar{u}, \bar{\mathbf{t}}^T, \bar{\boldsymbol{\theta}}^T]$ represent the initial lower and upper bound values for the variables given as $\underline{s}_m = 0, \bar{s}_m = 1, \underline{u} = r_o, \bar{u} = \max\{\bar{C}_m\}_{m \in \mathcal{M}}, \underline{t}_m = 0, \bar{t}_m = \bar{P}_m, \underline{\theta}_i = \psi_i^l$ and $\bar{\theta}_i = \psi_i^u$. This box is then successively branched and reduced across the iterations. Given a feasible reduced box B' , the aim is then to find a feasible

solution for \mathbf{w} and ϕ that satisfies (12), (13), (14), (18) and (20), which can be formulated as

$$\mathcal{P}_3 : \{\mathbf{w}_B, \phi_B\} = \text{find } \{\mathbf{w}, \phi\},$$

$$\text{s.t.} : \{\|\mathbf{w}_m\|^2 \leq s_m \min\{\bar{P}_m, \bar{t}_m\}, \forall m \in \mathcal{M}, \quad (24)$$

$$(13), (14), (18)\} \cap f_r(B),$$

where (24) is the convex intersection of (12) and (20). If the problem is feasible, we can calculate the l.b. and u.b. of η_e achieved by this box using (22) and (23), respectively, otherwise we can discard it from further partitioning. Due to its non-convex constraints (13), (14), and (18), the feasibility check of \mathcal{P}_3 is complicated. We express \mathcal{P}_3 as a transmit power minimization since it can greatly contribute to the EE

$$\mathcal{P}_4 : \{\mathbf{w}_B^*, \phi_B^*\} = \min_{\mathbf{w}, \phi} \|\mathbf{w}\|^2, \quad (25)$$

$$\text{s.t.} : \{(13), (14), (18), (24)\} \cap f_r(B).$$

If ϕ is determined, \mathcal{P}_4 can be expressed as

$$\mathcal{P}_5 : \mathbf{w}_B^* = \min_{\mathbf{w}} \|\mathbf{w}\|^2, \quad (26)$$

$$\text{s.t.} : |\mathbf{h}\mathbf{w}|^2 \geq \gamma\sigma^2, \quad (27)$$

$$\underline{s}_m \underline{t}_m \leq \|\mathbf{w}_m\|^2 \leq \bar{s}_m \min\{\bar{P}_m, \bar{t}_m\}, \forall m, \quad (28)$$

where $\gamma \triangleq 2^\alpha - 1$ is the SNR required for \underline{u} and $\mathbf{h}(\phi) = \mathbf{g} \text{diag}(\phi) \bar{\mathbf{H}}$ is the combined channel from all the active BSs, where $\bar{\mathbf{H}} = [\bar{\mathbf{s}}_1 \mathbf{H}_1, \dots, \bar{\mathbf{s}}_M \mathbf{H}_M]$. We can express the beamforming solution for each BS m as the matched filter

$$\mathbf{w}_m^* = s_m \sqrt{p_m} \frac{\mathbf{h}_m^H}{\|\mathbf{h}_m\|}, \quad (29)$$

therefore the cost function of \mathcal{P}_5 results in $\sum_m s_m p_m$. By inspecting constraint (27), we can obtain the following inequality

$$\sum_m s_m p_m \geq \frac{\gamma\sigma^2}{\|\mathbf{h}\|^2}, \quad (30)$$

since $\gamma\sigma^2 \leq |\sum_m \sqrt{p_m} s_m \mathbf{h}_m|^2 \leq (\sum_m s_m p_m) \|\mathbf{h}\|^2$. From (30), we see that in order to minimize the power consumption, the channel gain $\|\mathbf{h}(\phi)\|^2$ has to be maximized by ϕ . Then, we can allocate a power p_m for each BS with a feasible value that meets (28) and satisfies the minimum SNR requirement subject to the channel gain $\|\mathbf{h}\|_{\max}^2$ given by a feasible ϕ . This feasibility problem can be formulated as

$$\mathcal{P}_6 : \{\mathbf{p}_B\} = \text{find } \{\mathbf{p}\}, \quad (31)$$

$$\text{s.t.} : \sum_m s_m p_m \geq \frac{\gamma\sigma^2}{\|\mathbf{h}\|_{\max}^2}, \quad (32)$$

$$\underline{s}_m \underline{t}_m \leq p_m \leq \bar{s}_m \min\{\bar{P}_m, \bar{t}_m\}, \forall m \in \mathcal{M}. \quad (33)$$

First, we formulate the channel gain maximization problem as

$$\mathcal{P}_7 : \phi_B^* = \max_{\phi} \|\mathbf{g} \text{diag}(\phi) \bar{\mathbf{H}}\|^2 \quad (34)$$

$$\text{s.t.} (13), (14).$$

We expand the set \mathcal{F} in \mathcal{P}_7 to a convex circular region such that we can keep the box for further partitioning only if the expanded region contains at least one feasible solution, otherwise

we can discard it. By making $\mathbf{Q} = \text{diag}(\mathbf{g})\overline{\mathbf{H}}\overline{\mathbf{H}}^H\text{diag}(\mathbf{g}^H) \in S_+^I$ and introducing the auxiliary variables $\mathbf{x} \triangleq \phi^H$ and $\mathbf{X} \triangleq \mathbf{x}\mathbf{x}^H$, \mathcal{P}_7 is equivalent to

$$\mathcal{P}_8 : \{\mathbf{x}_B, \mathbf{X}_B\} = \max_{\mathbf{x}, \mathbf{X} \succeq 0} \text{tr}(\mathbf{Q}\mathbf{X}), \quad (35)$$

$$\text{s.t. } \mathbf{X} = \mathbf{x}\mathbf{x}^H, \quad (36)$$

$$\mathbf{X}_{ii} = 1, \forall i \in \mathcal{I}, \quad (37)$$

$$\arg(x_i) \in \mathcal{X}_i^B, \forall i \in \mathcal{I}, \quad (38)$$

where $\mathcal{X}_i^B \triangleq [l_i^B, u_i^B] \in [0, 2\pi], \forall i \in \mathcal{I}$, represents the search set for the argument of x_i in box B with lower and upper bounds l_i and u_i , respectively. Since θ can be directly recovered from \mathbf{x} , we can map the initial values of \mathcal{F}_i to \mathcal{X}_i as $l_i = (2\pi - \psi_i^u)$ and $u_i = (2\pi - \psi_i^l), \forall i \in \mathcal{I}$ and include them into T_0 instead of the arguments defined by \mathcal{F} . \mathcal{P}_8 is non-convex due to the rank-one constraint (36). If we drop it, \mathcal{P}_8 can be solved as a convex semidefinite problem (SDP). Then, from \mathbf{X}_B , we can extract an approximate solution for \mathbf{x}_B via eigenvalue decomposition or randomization methods [13], [14]. However, in this case, it is not guaranteed that the obtained \mathbf{x}_B will satisfy (38). On the other hand, we cannot drop (38), otherwise feasible solutions might be lost. Therefore, (36) and (38) are replaced by semidefinite and linear inequalities, respectively, derived from the relaxation of $\{\mathcal{X}_i^B\}_{i \in \mathcal{I}}$.

B. Enhanced SDP relaxation

Each argument search set $\mathcal{X}_i \triangleq [l_i, u_i] \subset [0, 2\pi]$ can be expanded to its circular segment defined as $\tilde{\mathcal{X}}_i = \{\tilde{x}_i \in \mathbb{C} \mid \Re(a_i^* \tilde{x}_i) \geq \cos(\frac{u_i - l_i}{2}), |\tilde{x}_i| \leq 1\}$, where $a_i \triangleq e^{\frac{u_i + l_i}{2}}, \forall i \in \mathcal{I}$ [11]. Also, $|\tilde{x}_i| \leq 1$ can be realized implicitly by relaxing (36) to $\tilde{\mathbf{X}} \succeq \tilde{\mathbf{x}}\tilde{\mathbf{x}}^H$. Then \mathcal{P}_8 is relaxed as

$$\mathcal{P}_9 : \{\tilde{\mathbf{x}}_B, \tilde{\mathbf{X}}_B\} = \max_{\tilde{\mathbf{x}}, \tilde{\mathbf{X}} \succeq 0} \text{tr}(\mathbf{Q}\tilde{\mathbf{X}}), \quad (39)$$

$$\text{s.t. } \tilde{\mathbf{X}} \succeq \tilde{\mathbf{x}}\tilde{\mathbf{x}}^H, \quad (40)$$

$$\Re(a_i^* \tilde{x}_i) \geq \cos(\frac{u_i - l_i}{2}), \forall i \in \mathcal{I}, \quad (41)$$

$$\tilde{\mathbf{X}}_{ii} = 1, \forall i. \quad (42)$$

The newly introduced constraints (40) and (41) enable solving \mathcal{P}_9 with an SDP solver such as CVX [15]. Branching over $\arg(x_i)$ is based on the fact that if for each vertex i , the width of $\mathcal{X}_i : (u_i - l_i) \rightarrow 0$ then $|\tilde{x}_i| \rightarrow 1$, for any feasible solution \tilde{x}_i within the relaxed circular region $\tilde{\mathcal{X}}_i$. Also, if $\tilde{\mathbf{x}}$ is the feasible solution of \mathcal{P}_9 , with $|\tilde{x}_i| = 1, \forall i \in \mathcal{I}$, then $\tilde{\mathbf{x}}$ is also feasible for \mathcal{P}_8 [11]. That means that \mathcal{X} has to be successively branched across BRnB iterations in order to move $\tilde{\mathbf{x}}$, thus ϕ , towards the circle contour, i.e., satisfying (13) and (14). Therefore, the feasible value for the channel gain is $\|\mathbf{h}\|_{\max}^2 = \tilde{\mathbf{x}}^H \mathbf{Q} \tilde{\mathbf{x}}$, where \tilde{x}_i' is the projection of \tilde{x}_i onto the unit-circle. Furthermore, to decide the edge to branch a box B into B_- and B_+ , the candidate among the edges $n = N_s + 1, \dots, N_t$, is the phase i given by $i_{\max} = \arg \max_{i \in \mathcal{I}} \{|\tilde{x}_i' - \tilde{x}_i|\}$, which is then compared with the edges defined by the monotonic variables u, s , and t and then we take the longest. \mathcal{P}_1 can be optimally solved following Algorithm 1.

Algorithm 1: BRnB algorithm for solving \mathcal{P}_1

Result: $\eta^*, \mathbf{s}, \phi, \{\mathbf{w}_m\}$

initialize $T_0 = [\mathbf{p}, \mathbf{q}]$ for \mathbf{s}, u, t and $\arg(\mathbf{x})$, reduce and assign it to the box set $\mathcal{B}_0 \leftarrow f_r(T_0)$, $\eta_e^{glb} = 0$, and $i = 1$

while $(\eta_{e,i}^{gub} - \eta_{e,i}^{glb})/\eta_{e,i}^{gub} > \epsilon_1$ **do**

select box B that provides the highest upper bound

select edge $n = \arg \max_{m=1, \dots, N_t} (q_m - p_m)$ giving priority to

\mathbf{s} until $\underline{s} = \bar{s}$ and branch B into B_1 and B_2 using (21)

for $r = 1 : 2$ **do**

reduce B_r to B_r' via bisection with precision ϵ_2

if reduction is feasible **then**

if $\eta_e^{lub}(B_r') > \eta_e^{glb}$ **then**

solve \mathcal{P}_9 and get $\tilde{\mathbf{x}}$ and ϕ^B

if infeasible **then** discard B_r'

else

solve \mathcal{P}_6 and get \mathbf{p}

compute $\|\mathbf{h}\|_{\max}^2$

compute \mathbf{w}_m^B using (29)

compute $\eta_e^{lub}(B_r')$ using (22)

compute $\eta_e^{lub}(B_r')$ using (23)

update $\eta_{e,i}^{glb} \leftarrow \max(\eta_{e,i-1}^{glb}, \eta_e^{lub}(B_r'))$

else discard B_r' , new optimal is not here

else discard B_r , no feasible points

update box set $\mathcal{B}_i \leftarrow (\mathcal{B}_{i-1} \setminus B) \cup \{B_r' \mid \eta_e^{lub}(B_r') \geq \eta_{e,i}^{glb}\}$

update $\eta_{e,i}^{gub} \leftarrow \max_{b \in \mathcal{B}_i} (\eta_e^{lub}(b))$ and $i \leftarrow i + 1$.

IV. SIMULATION RESULTS

We consider a setup in an area \mathcal{A}_B of $800\text{m} \times 800\text{m}$, where $M = 4$ BSs, each with $N = 3$ antennas, located at the vertices and at a height of $H_{B,m} = 4\text{m}, \forall m$, aim to serve a ground UE located at an inner area \mathcal{A}_U of $\frac{800}{3}\text{m} \times \frac{800}{3}\text{m}$ via a hovering aerial-RIS. The position of each BS m is denoted by $\mathbf{v}_{B,m}$, the position of the UE is $\mathbf{v}_U = [x, y, 0]$, and the position of the first element of the RIS is $\mathbf{v}_R = [400, 400, H_R]$, with $H_R = 50\text{m}$ being the altitude of the UAV. Similar as in [4], we consider uniform-linear arrays (ULAs) at both the BSs and the RIS, but extending to uniform planar array (UPA) is also possible. The ULAs have response

$$\alpha(L, d_a, \Omega) = \left[1, e^{-j2\pi \frac{d_a}{\lambda} \sin \Omega}, \dots, e^{-j2\pi \frac{d_a}{\lambda} (L-1) \sin \Omega} \right]^T,$$

where L is the number of elements, λ is the wavelength, d_a is the antenna interspacing, and Ω is the reference angle. We assume $d_a = \lambda/2$ at each BS and $d_a = \lambda/10$ at the RIS. The channels are Rician with path-losses BS $_m$ -RIS and RIS-UE $\beta_{B,m} = \frac{\beta_0}{\|\mathbf{v}_R - \mathbf{v}_{B,m}\|^2}$ and $\beta_q = \frac{\beta_0}{\|\mathbf{v}_R - \mathbf{v}_U\|^2}$, respectively [4], where $\beta_0 = -40\text{dB}$ is the channel power at the distance of 1m. The channels are given by $\mathbf{H}_m = \sqrt{\beta_{B,m}} \left(\sqrt{\rho_{B,m}}/(\rho_{B,m} + 1) \hat{\mathbf{H}}_m + \sqrt{1/(\rho_{B,m} + 1)} \hat{\mathbf{H}}_m \right)$, and $\mathbf{g} = \sqrt{\beta_q} \left(\sqrt{\rho_q}/(\rho_q + 1) \hat{\mathbf{g}}_k + \sqrt{1/(\rho_q + 1)} \tilde{\mathbf{g}}_k \right)$, where ρ_B , and ρ_q are Rician factors with value of 10, and $\hat{\mathbf{H}}_m = \alpha(I, \frac{\lambda}{10}, \Omega_{\text{AoA},m}) \alpha^H(N, \frac{\lambda}{2}, \Omega_{\text{AoD},m})$ and $\hat{\mathbf{g}} = \alpha^H(I, \frac{\lambda}{10}, \Omega_{\text{AoD},\text{RIS}})$. $\Omega_{\text{AoA},m}$ and $\Omega_{\text{AoD},m}$ are the

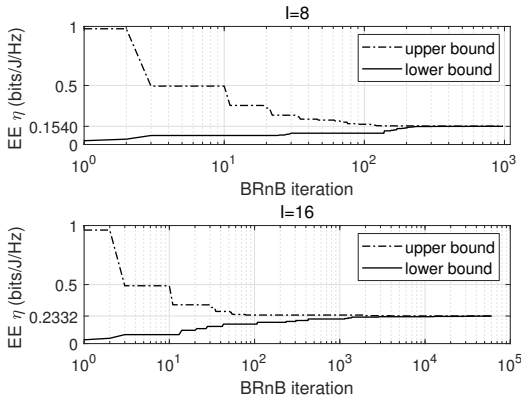


Fig. 2. Energy Efficiency Optimization using Algorithm 1.

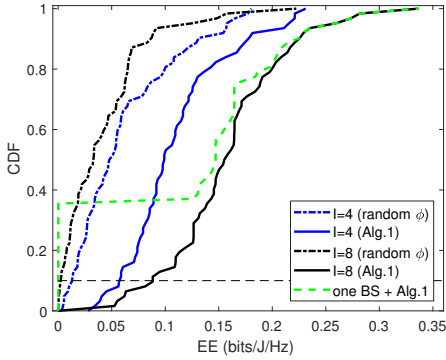


Fig. 3. Comparison of EE for different RIS and BS configurations

AoA and AoD of the signal from BS m to the RIS, and $\Omega_{\text{AoD,RIS}}$ is the AoD of the signal from the RIS to the UE. \mathbf{H}_m and $\tilde{\mathbf{g}}$ represent scattering whose elements follow $\mathcal{CN}(0, 1)$. The rest of parameters are set as $\sigma^2 = -110$ dBm, $r_o = 1$ bit/s/Hz, $P_E = 10$ mW, $\psi_i^l = \pi$ and $\psi_i^u = 2\pi, \forall i$, $\bar{P}_m = 2$ W, $\bar{C}_m = 4$ bit/s/Hz, $P_{\text{BS}}^{\text{run}} = 5$ W, $P_{\text{BS}}^{\text{sl}} = 1$ W, $\eta_{\text{PA}} = 0.4$, $\eta_{\text{FH}} = 0.3$, and Algorithm precision $\epsilon_1 = 10^{-3}$ and $\epsilon_2 = 10^{-5}$. Fig. 2 presents the algorithm convergence for a particular channel realization and two different numbers I of RIS elements. The UE position is the same in both cases. As seen, in each case, the lower and upper bounds of η converge to the same value. However, since the dimension of the problem in the second case, $N_s = 2M + I + 1 = 25$, is higher than in the first case, $N_s = 17$, BRnB needs more iterations for a feasible solution within the given precision. Also, on the convergence, we see that the EE when $I = 16$ is approximately 50% higher than when $I = 8$. This is because with a larger RIS, less transmit power and only one BS were needed, whereas two BSs were needed when $I = 8$. In each case, the Algorithm selected the BSs with the highest channel gains. Fig. 3 compares the EE cumulative density function (CDF) from 100 random locations of the UE in \mathcal{A}_U when $I = 4$ and $I = 8$, and for the cases 1) the system is fully optimized with Algorithm 1, 2) the BS selections are optimized but the RIS phase-shifts are set randomly, and

3) selection of only one BS. In this case, the trend is the same as in Fig. 2, where a larger RIS provides higher EE for every UE location. We observe a performance loss caused by random RIS phase-shifts, which is higher for the larger RIS. Also, even though the one BS setup is the best option in some cases, it can suffer from outage. For instance, 40% of the cases were infeasible due to QoS and power constraints, whereas this problem is solved by our cooperative scheme.

V. CONCLUSION

In this paper, we proposed an aerial-RIS-aided cooperative wireless communication system for emergency relief and studied its energy efficiency (EE) for the single user case considering RIS phase-shifts, QoS, transmit power and fronthaul capacity constraints. We proposed a BRnB algorithm to maximize the EE by optimizing the BS and RIS beamformers jointly with the selection of the BSs that participate in the transmission. It was shown that the EE increases with the number of RIS elements as well as our scheme has better EE and outage performance than the single BS case.

REFERENCES

- [1] S. Chandrasekharan et al., "Designing and implementing future aerial communication networks," *IEEE Commun. Mag.*, vol. 54, no. 5, pp. 26-34, 2016.
- [2] A. Al-Hourani, S. Kandeepan and S. Lardner, "Optimal LAP Altitude for Maximum Coverage," *IEEE Wireless Commun. Letters*, vol. 3, no. 6, pp. 569-572, 2014.
- [3] C. Huang, A. Zappone, G. C. Alexandropoulos, M. Debbah and C. Yuen, "Reconfigurable Intelligent Surfaces for Energy Efficiency in Wireless Communication," *IEEE Trans. Wireless Commun.*, vol. 18, no. 8, pp. 4157-4170, 2019.
- [4] H. Lu, Y. Zeng, S. Jin and R. Zhang, "Enabling Panoramic Full-Angle Reflection Via Aerial Intelligent Reflecting Surface," *IEEE Int. Conf. on Commun. Workshops*, pp. 1-6, 2020.
- [5] A. Ptilakis et al., "A Multi-Functional Reconfigurable Metasurface: Electromagnetic Design Accounting for Fabrication Aspects," *IEEE Trans. Antennas Propag.*, vol. 69, no. 3, pp. 1440-1454, 2021.
- [6] T. Zhou, K. Xu, X. Xia, W. Xie and J. Xu, "Achievable Rate Optimization for Aerial Intelligent Reflecting Surface-Aided Cell-Free Massive MIMO System," *IEEE Access*, vol. 9, pp. 3828-3837, 2021.
- [7] T. Do, G. Kaddoum, T. Nguyen, D. Benevides and Z. Haas, "Aerial Reconfigurable Intelligent Surface-Aided Wireless Communication Systems," 2021, *arXiv:2106.05380*.
- [8] X. Yu, D. Xu and R. Schober, "Optimal Beamforming for MISO Communications via Intelligent Reflecting Surfaces," *IEEE Int. Workshop on Signal Process. Advances in Wireless Commun.*, pp. 1-5, 2020.
- [9] K. Nguyen, Q. Vu, M. Juntti and L. Tran, "Energy Efficiency Maximization for C-RANs: Discrete Monotonic Optimization, Penalty, and ℓ_0 -Approximation Methods," *IEEE Trans. Signal Process.*, vol. 66, no. 17, pp. 4435-4449, 2018.
- [10] H. Tuy, M. Minoux and N. Hoai-Phuong, "Discrete Monotonic Optimization with Application to a Discrete Location Problem," *SIAM J. Optim.*, vol. 17, no. 1, pp. 78-97, 2006.
- [11] L. Cheng, D. Zhibin, W. Zhang and S. Fang, "Argument division based branch-and-bound algorithm for unit-modulus constrained complex quadratic programming," *J. Glob. Optim.*, vol. 70, no. 1, pp. 171-187, 2018.
- [12] I. Ashraf, F. Boccardi, and L. Ho, "SLEEP mode techniques for small cell deployments," *IEEE Commun. Mag.*, vol. 49, no. 8, pp. 72-79, 2011.
- [13] A. So, J. Zhang, and Y. Ye, "On approximating complex quadratic optimization problems via semidefinite programming relaxations," *Math. Program.*, vol. 110, no. 1, pp. 93-110, 2007.
- [14] Z. Luo, W. Ma, A. So, Y. Ye and S. Zhang, "Semidefinite Relaxation of Quadratic Optimization Problems," *IEEE Signal Process. Mag.*, vol. 27, no. 3, pp. 20-34, 2010.
- [15] CVX Research, Inc., "CVX: Matlab Software for Disciplined Convex Programming, version 2.0," 2012, <http://cvxr.com/cvx>.